teins (which bind active GTP-bound Rho) in triplicate and incubated at 4 °C for 30 min with vigorous shaking. Active Rho levels were determined by subsequent incubations with anti-Rho antibody and secondary horseradish peroxidase-conjugated antibody for 45 min each at room temperature. After adding developing solution, the level of active Rho was determined by measuring absorbance at 490 nm using an ELISA plate reader. Equal loading of total RhoA protein at each time point was determined via immunoblotting using anti-RhoA antibody as described above. Experiments were repeated at least three times.

2.8. Immunofluorescence

Huh-7 cells were transfected with siRNA targeting *ARHGAP5* or negative control siRNA or were left untreated. Cells were harvested 48 h after transfection, suspended for 1 h in DMEM containing 1% FCS and then plated on glass slides coated with fibronectin for 10, 20, 40, 60 or 180 min. Cells were fixed for 10 min in 3.7% formaldehyde, permeabilized for 2 min in 1% Triton X-100 and incubated for 1 h with a blocking buffer (phosphate-buffered saline containing 3% bovine serum albumin). The cells were then incubated for 1 h at room temperature with anti-p190-B RhoGAP monoclonal antibody diluted 1:200 in blocking buffer. Fluorescein isothiocyanate (FITC)-conjugated anti-mouse IgG (Cappel, Aurora, OH, USA) was used to detect the primary antibody. Actin filaments and nuclei were counterstained with rhodamine-phalloidin (Molecular Probes, Eugene, OR, USA) and 4',6-diamidino-2-phenylindole (DAPI; Sigma–Aldrich), respectively.

2.9. Monolayer wound healing assay

Huh-7 cells were transfected with siRNA targeting *ARHGAP5* or negative control siRNA or left untreated. After 24 h, cells in DMEM with 1% FCS were seeded on glass slides coated with fibronectin and allowed to adhere overnight.

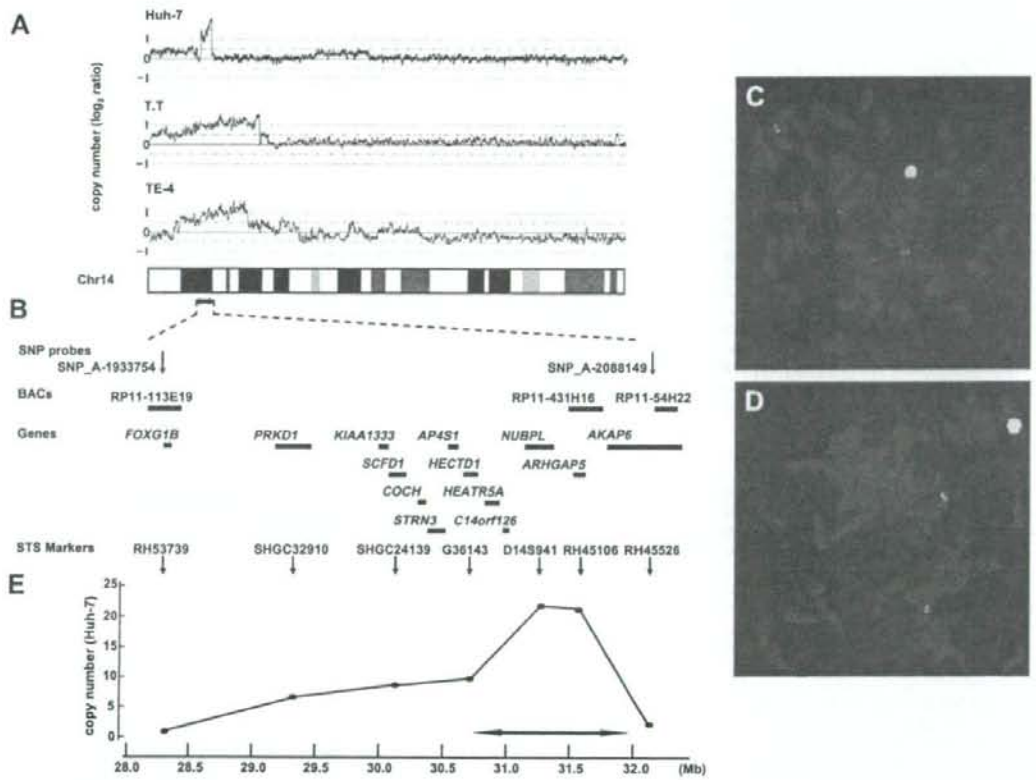

Fig. 1. Map of the amplicon at 14q12. (A) Copy number profiles for chromosome 14 in Huh-7, T.T and TE-4 cells. Copy number values were determined by GeneChip Mapping 250 K array analyses. (B) The positions of the Affymetrix SNP probes, three BACs used as probes for FISH experiments, the 13 genes within the 14q12 amplicon, and the seven STS markers used for real-time quantitative PCR on genomic DNA are shown according to the UCSC genome database (http://genome.ucsc.edu/). (C and D) Representative images of two-color FISH on metaphase chromosomes from Huh-7 cells using BACs: paired RP11-431H16 (green; C) and RP11-113E19 (red; C), or paired RP11-431H16 (green; D) and RP11-54H22 (red; D). (E) Copy numbers at the seven STS marker loci in Huh-7 cells as measured by real-time quantitative PCR with reference to LINE-1 controls. Values are normalized such that the copy number in genomic DNA derived from normal lymphocytes has a value of 2. The smallest region of amplification is indicated (arrow).

We scratched wounds in the cell monolayer using a sterile 200-μl pipet tip, rinsed the cells with phosphate-buffered saline and added DMEM containing 10% FCS with or without mitomycin C (10 μg/ml, Nacalai Tesque, Kyoto, Japan). Cells were allowed to migrate into the wound for 0, 12, or 24 h before fixation. Cells were stained with Giemsa stain (Nacalai Tesque) or were triple-labeled with anti-p190-B RhoGAP, rhodamine-phalloidin and DAPI as described above. Wound widths were measured in three randomly chosen regions. Experiments were repeated at least three times.

2.10. Statistical analysis

Analysis of variance (ANOVA) was performed using SPSS 15.0 software (SPSS Inc., Chicago, IL, USA). *P* values of <0.05 were considered significant.

3. Results

3.1. Detection of 14q12 amplicon in HCC and ESCC cell lines by array analyses

We screened for DNA copy number aberrations in 10 HCC cell lines and 10 ESCC cell lines using GeneChip Mapping 250 K array analysis. Of the 20 cell lines, one HCC cell line, Huh-7, and two ESCC cell lines, T.T and TE-4, commonly exhibited copy number gains at chromosomal region 14q12 (Fig. 1A). In particular, Huh-7 cells showed a high-level gain indicative of amplification in a narrow region on 14q12 between the positions recognized by the Affymetrix SNP_A-1933754 and SNP_A-2088149 probes. To confirm amplification in Huh-7 cells, we performed FISH analyses using BACs RP11-113E19, RP11-431H16 and RP11-54H22 as probes (Fig. 1B–D). BAC RP11-431H16 generated strong signals as a small homogeneously staining region (HSR), indicating amplification (Figs. 1C, D). In contrast, BACs RP11-113E19 or RP11-54H22 did not show a HSR pattern, indicating their positions outside the amplicon (Fig. 1C and D). Furthermore, we determined gene dosages in Huh-7 cells at the STS markers RH53739, SHGC32910, SHGC24139, G36143, D14S941, RH45106, and RH45526 loci by real time quantitative PCR. (Fig.1B and E). The highest copy number was observed at the D14S941 and RH45106 loci. Taken together, we defined the smallest region of amplification between markers G36143 and RH45526. The extent of the amplicon was estimated to be 1.2 Mb. This region includes four known or predicted protein-coding genes, *HEATR5A*, *c14orf126*, *NUBPL*, and *ARHGAP5*.

3.2. Identification of candidate target genes in the 14q12 amplicon

The 14q12 region may harbor one or more genes (henceforth called 'target genes') that, when activated by amplification, play a role in carcinogenesis. A common criterion for designating a gene as a putative target is that amplification leads to its overexpression [8]. Using real-time quantitative PCR, we determined mRNA levels of all four genes within the amplicon in the 10 HCC cell lines and 10 ESCC cell lines. Among the four genes, *HEATR5A* and *ARHGAP5* were commonly overexpressed in Huh-7, T.T and TE-4 cells, the cell lines that were found to have copy number gains at 14q12 (Fig. 2A). These findings identified *ARHGAP5*, which encodes p190-B RhoGAP, as one of candidate target genes for the 14q12 amplicon.

We determined copy numbers of *ARHGAP5* in the 10 HCC and 10 ESCC cell lines by real-time quantitative PCR (Fig. 2B). Copy number changes were counted as gains if the results of the analysis for a given tumor cell type exceeded the twofold levels of the gene in normal cells. A copy number gain of *ARHGAP5* was observed in six (30%) of the 20 cell lines: Huh-7, T.T, KYSE140, TE-4, TE-6 and TE-10.

We examined the expression of p190-B RhoGAP protein in 4 HCC and 4 ESCC cell lines by immunoblot analysis. As shown in Fig. 2C, expression levels of p190-B RhoGAP were higher in cell lines exhibiting copy number gains of *ARHGAP5* (Huh-7, T.T, KYSE140, TE-4 and TE-10) than other cell lines that did not show gains (SNU354, Huh-1 and PLC/PRF/5).

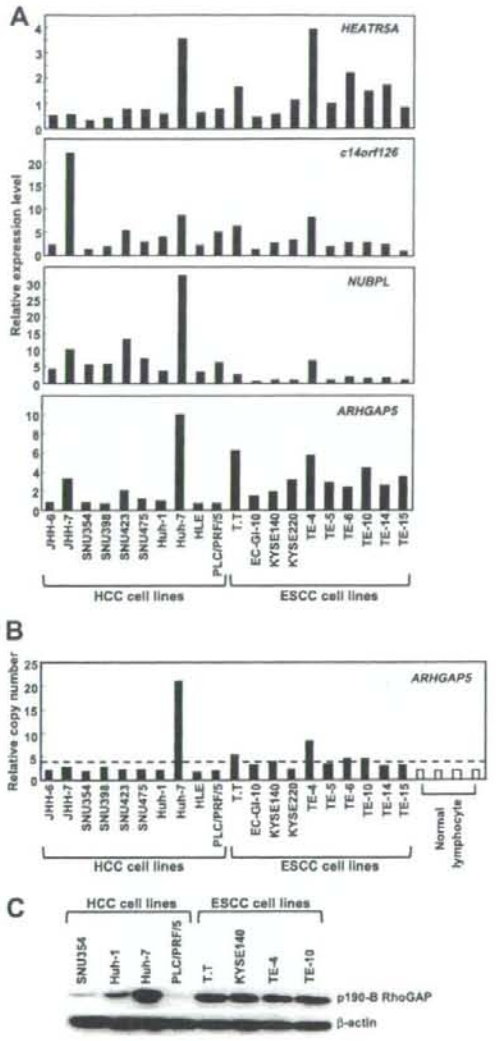

Fig. 2. Amplification and overexpression of *ARHGAP5* in Huh-7, T.T and TE-4 cell lines. (A) Relative expression levels of four genes (*HEATR5A*, *c14orf126*, *NUBPL* and *ARHGAP5*) within the 14q12 amplicon in 10 HCC and 10 ESCC cell lines as evaluated by real-time quantitative PCR. Results are presented as expression levels of each gene relative to a reference gene (*GAPDH*) to correct for variations in the amount of RNA. (B) Copy numbers at the *ARHGAP5* locus (the STS marker RH45106) in 10 HCC cell lines, 10 ESCC cell lines and four normal peripheral blood lymphocytes as measured by real-time quantitative PCR with reference to LINE-1 controls. Values are normalized such that the average copy number in genomic DNA derived from four normal lymphocytes has a value of 2. A value of 4, which is a twofold increase in copy number of normal lymphocytes, was used to determine the cut-off value for copy number gain, shown as a dotted line. (C) Levels of p190-B RhoGAP and β-actin, an internal control, determined by immunoblotting in 4 HCC and 4 ESCC cell lines.

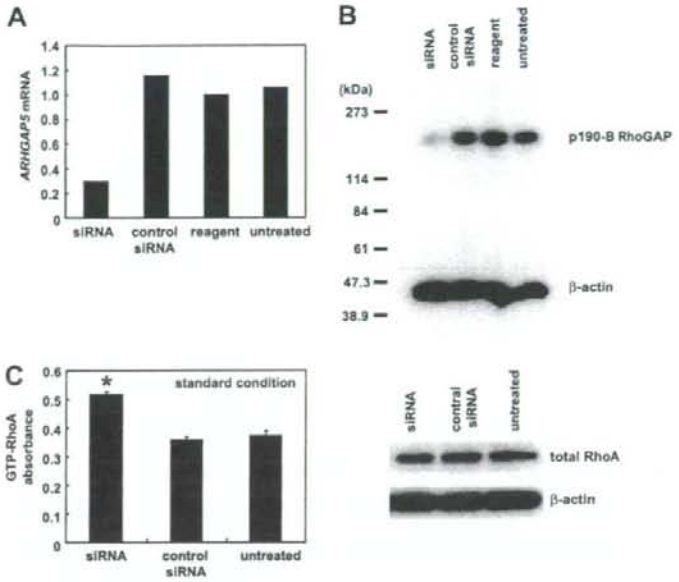

Fig. 3. Knockdown of *ARHGAP5* increases RhoA activity. (A) Relative expression levels of *ARHGAP5* mRNA as determined by real-time quantitative PCR. Huh-7 cells were treated with siRNA targeting *ARHGAP5*, negative control siRNA or transfection agent alone. Untreated cells were maintained under identical experimental conditions. Results are presented as a ratio between the expression level of *ARHGAP5* and that of a reference gene (*GAPDH*) to correct for variation in the amount of RNA. Relative expression levels were normalized such that the ratio in untreated cells was 1. (B) Levels of p190-B RhoGAP and β-actin, an internal control, determined by immunoblotting. (C) (*left*) Levels of RhoA activity under standard culture conditions (DMEM containing 10% FCS). RhoA activity was measured using a G-LISA kit (see Methods section). Values are represented as the mean ± S.D. Differences were analyzed by ANOVA ($^{*}P < 0.05$). (*right*) Total RhoA and β-actin were determined by immunoblotting.

3.3. Regulation of RhoA activity by p190-B RhoGAP in Huh-7 cells

To investigate the biological function of p190-B RhoGAP in HCC cells, knockdown of *ARHGAP5* expression in Huh-7 cells was carried out using RNAi. Following treatment of Huh-7 cells with siRNA targeting *ARHGAP5*, we observed a decrease in both *ARHGAP5* mRNA and p190-B RhoGAP protein levels relative to what was observed for cells receiving control siRNA, transfection agent alone or left untreated (Fig. 3A and B). Because p190-B RhoGAP negatively regulates RhoA activity, we examined the effect of the siRNA-mediated knockdown of *ARHGAP5* on RhoA activity. Huh-7 cells were treated with *ARHGAP5* siRNA or control siRNA or were left untreated. Cells were then cultured in DMEM containing 10% FCS for 48 h under standard conditions. RhoA activity levels were higher in cells treated with *ARHGAP5* siRNA than in cells treated with control siRNA or in untreated cells, whereas total RhoA levels were similar among the three groups (Fig. 3C). These findings suggest that overexpression of *ARHGAP5* contributes to downregulation of RhoA activity in Huh-7 cells.

3.4. Regulation of cell spreading by p190-B RhoGAP in Huh-7 cells

It is known that integrin-mediated adhesion regulates the activity of p190-B RhoGAP and RhoA [3,9]. We therefore examined the function of p190-B RhoGAP when Huh-7 cells were plated on fibronectin, a specific ligand for α5β1 integrin. Huh-7 cells treated with *ARHGAP5* siRNA or control siRNA or left untreated were suspended and plated on fibronectin. Prior to and during plating, cells were maintained in DMEM containing 1% FCS. Adhesion to fibronectin regulated RhoA activity in a triphasic or biphasic manner (Fig. 4A). Prior to plating (0 min), RhoA activity was significantly higher in *ARHGAP5* siRNA-treated cells than in control siRNA-treated cells or untreated cells. In *ARHGAP5* siRNA-treated cells, RhoA activity rapidly and transiently decreased (20 min). This initial decline was followed by an increase that peaked at 60 min. In the final phase, RhoA activity gradually decreased. In control siRNA-treated cells or untreated cells, an initial period of low RhoA activity was followed by a slight increase that peaked between 40–60 min and then returned to basal level. RhoA activity was significantly higher in *ARHGAP5* siRNA-treated cells than control siRNA-treated cells or untreated cells between 40 and 180 min. During the experimental period, expression of p190-B RhoGAP was continuously knocked down by *ARHGAP5* siRNA and total RhoA levels were similar among the three groups (Fig. 4A).

Because RhoA affects cell motility by stimulating reorganization of actin, we examined whether p190-B RhoGAP regulates the spreading of Huh-7 cells on fibronectin. Using immunofluorescence, we observed morphological changes in Huh-7 cells during attachment and spreading on fibronectin (Fig. 4B). Phalloidin staining revealed that *ARHGAP5* siRNA-treated cells exhibited more robust actin stress fibers but less membrane ruffling and protrusion at the cell periphery than control siRNA-treated cells or untreated cells. The actin stress fiber formation and reduced membrane ruffling and protrusion observed in *ARHGAP5* siRNA-treated cells corresponded with higher RhoA activity (Fig. 4)

p190-B RhoGAP was expressed diffusely in the cytoplasm of control siRNA-treated cells and untreated cells, whereas it was hardly detected in *ARHGAP5* siRNA-treated cells. We found that p190-B RhoGAP had partially translocated to the membrane protrusions in control siRNA-treated cells and untreated cells by 40 min after plating (Fig. 4B). Taken together, these findings suggest that RhoA inactivation by p190-B RhoGAP results in inhibition of actin stress fiber formation, enhanced membrane ruffling and protrusion and promotion of cell spreading on fibronectin.

3.5. Regulation of cell migration by p190-B RhoGAP in Huh-7 cells

To investigate the role of p190-B RhoGAP in cell motility, we performed a monolayer wound healing assay. Wound closure was delayed in *ARHGAP5* siRNA-treated cells relative to control siRNA-treated cells or untreated cells, whether cultured in the presence of mitomycin C or in its absence (Figs. 5A–E). Mitomycin C blocks mitosis and thus allows analysis of cell migration in the absence of cell proliferation. These results show that cell migration, rather than cell proliferation, is the major factor

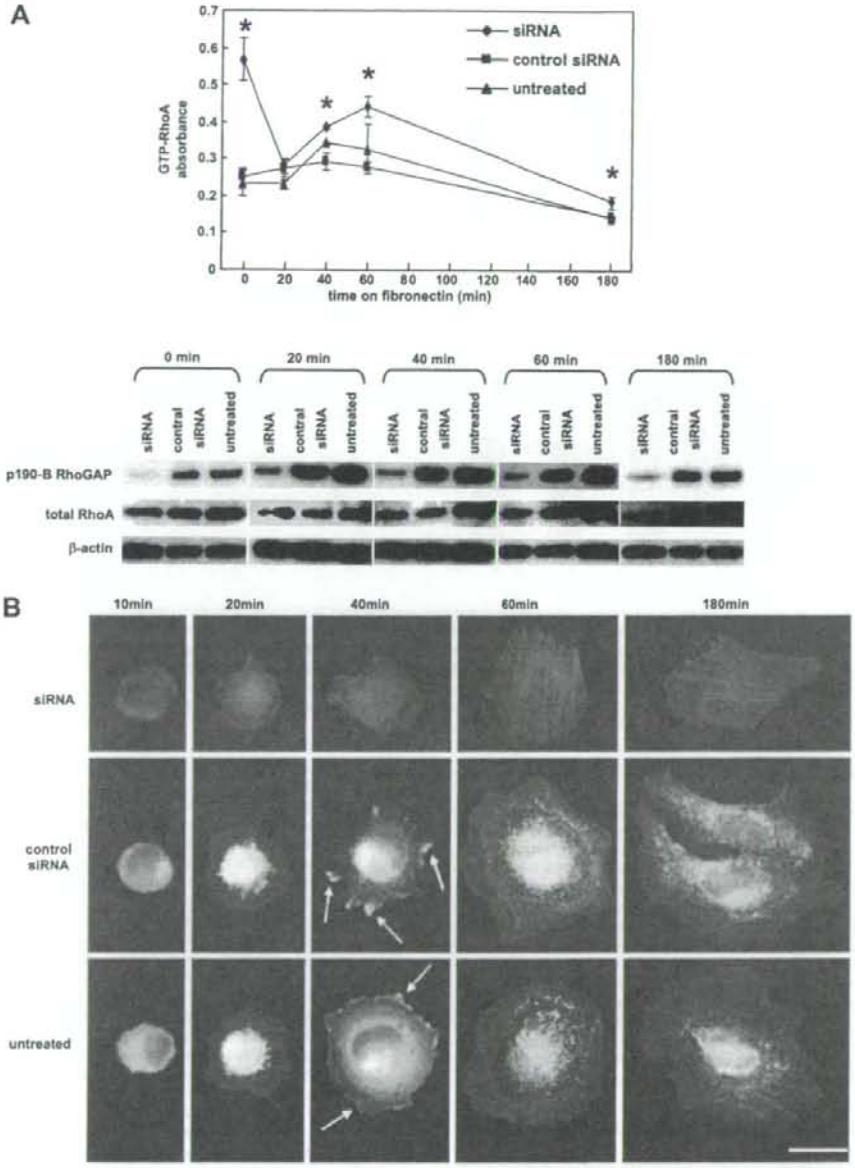

Fig. 4. Knockdown of *ARHGAP5* inhibits Huh-7 cell spreading on fibronectin. (A) Time course of changes in RhoA activity (*upper*) and levels of p190-B RhoGAP and total RhoA (*lower*). Huh-7 cells treated with siRNA targeting *ARHGAP5* or control siRNA or left untreated were plated on fibronectin as described in Materials and Methods and harvested at the indicated time points. Values of RhoA activity are represented as the mean ± SD. Differences were analyzed by ANOVA ($^{*}P < 0.05$). Levels of p190-B RhoGAP, total RhoA and β-actin were determined by immunoblotting. (B) Time course of cell spreading on fibronectin. Huh-7 cells treated with siRNA targeting *ARHGAP5* or control siRNA or left untreated were plated on fibronectin, fixed at the indicated time points and then triple-labeled with anti-p190-B RhoGAP, rhodamine-conjugated phalloidin and DAPI to reveal p190-B RhoGAP (green), actin filaments (red), and nuclei (blue), respectively. Arrows indicate p190-B RhoGAP on membrane protrusions. Scale bar = 10 μm.

in the retarded wound repair process in *ARHGAP5* siRNA-treated cells. Wound edge cells in *ARHGAP5* siRNA-treated cells had more abundant actin stress fibers but less membrane ruffling and protrusion at the leading edge than control siRNA-treated or untreated cells (Figs. 5F–H). p190-B RhoGAP translocated to the membrane protrusions of control siRNA-treated or untreated cells at the edge of the wound, but not in *ARHGAP5*-siR-

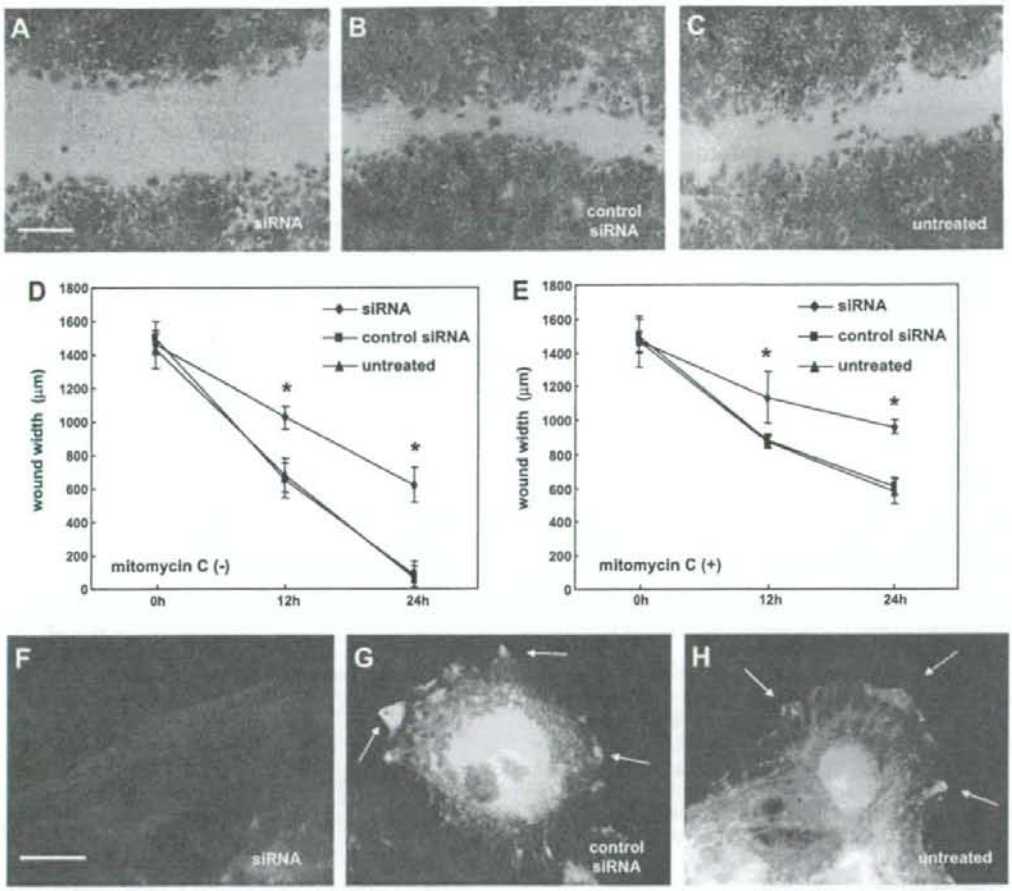

Fig. 5. Knockdown of *ARHGAP5* inhibits migration in Huh-7 cells. Monolayer wound healing assay in Huh-7 cells transfected with siRNA targeting *ARHGAP5* (A, F) or control siRNA (B and G), or left untreated (C and H). Cells were cultured in the absence (A–D, F–H) or presence (E) of mitomycin C. (A–C) Cells were allowed to migrate into a monolayer wound for 24 h and afterward stained with Giemsa stain. Original magnifications: 40×. Scale bar = 500 μm. (D and E) Cells were cultured in the absence (D) or presence (E) of mitomycin C. Wound widths were measured in three randomly chosen regions at the indicated time after wounding. Values are represented as the mean ± SD. Differences were analyzed by ANOVA (*$P < 0.05$). (F–H) Wound edge cells were triple-labeled with anti-p190-B RhoGAP, rhodamine-conjugated phalloidin and DAPI to reveal p190-B RhoGAP (green), actin filaments (red) and nuclei (blue), respectively. Arrows indicate p190-B RhoGAP on membrane protrusions. Scale bar = 10 μm.

NA cells. Taken together, these observations suggest that the inhibition of RhoA activity by p190-B RhoGAP promotes cell movement and formation of membrane protrusions in migrating cells.

4. Discussion

We report here the amplification of *ARHGAP5* in HCC and ESCC cell lines. We undertook a molecular definition of the amplicon at 14q12 that is present in HCC and ESCC cell lines. The amplification at 14q12 has been reported in various types of cancers, including HCC [10], ESCC [7], nasopharyngeal carcinoma [11] and non-squamous cell lung carcinoma [12], although the frequency of 14q12 gain is low in primary HCC (4–6%) [10,13]. The range of the amplicon varies among these tumors, and their boundaries have not been determined in each case. Moreover, the target oncogene(s) in the amplified regions have not been fully identified. Here we defined the amplified regions in one HCC and two ESCC cell lines and narrowed the site of the amplification to a relatively short section. Among the four genes within the smallest region of the amplification, only *HEATR5A* and *ARHGAP5* were overexpressed in all the tested lines exhibiting copy number gains in the region; hence they are thought to be candidate targets in the amplicon. Of the two genes, we chose to focus further analysis on *ARHGAP5* because its protein product, p190-B RhoGAP, is purported to play an important role in dynamic cellular processes by regulating RhoA activity, while little is known about *HEATR5A*. During the preparation of this manuscript, amplification of *ARHGAP5* was reported in Huh-7 cells [14].

Although several studies have suggested an association of p190-B RhoGAP with tumors [15–17], its biological function in cancer cells is poorly understood. Therefore, using siRNA, we studied its function in Huh-7 cells, the HCC cell line that exhibited the most remarkable copy number gain and overexpression of *ARHGAP5*. We found that p190-B RhoGAP negatively regulates RhoA activity in Huh-7 cells cultured in medium containing 10% FCS and plated on fibronectin. Adhesion to fibronectin regulated RhoA activity in a triphasic or biphasic manner, as previously reported in fibroblasts [18,19]. Although some RhoA activity is required for migration, possibly to maintain sufficient adhesion to the substrate, high activity inhibits movement [19–22]. Our results showed that RhoA inactivation by p190-B RhoGAP results in inhibition of actin stress fiber formation, enhanced membrane ruffling and protrusion, and promotion of spreading and migration of Huh-7 cells. These findings are in agreement with results obtained from previous studies. A dominant negative (loss-of-function) p190-B RhoGAP mutation elevates RhoA activity in fibroblasts cultured on fibronectin and inhibits their migration, whereas overexpression of wild-type p190-B RhoGAP decreases RhoA activity, promotes the formation of membrane protrusions and enhances mobility [19]. Activation of β1 integrin signaling stimulates tyrosine phosphorylation of p190-B RhoGAP and promotes membrane protrusion at invadopodia in a melanoma cell line [17]. p190-B RhoGAP is also involved in invasion by breast cancer cells [15].

In conclusion, we have identified *ARHGAP5* as a probable target for the amplification at 14q12 detected in a subgroup of HCCs and ESCCs. Our results indicate that p190-B RhoGAP, the protein product of *ARHGAP5*, promotes cell spreading and migration in Huh-7 cells. Further studies are needed to determine the importance of *ARHGAP5* and p190-B RhoGAP in the development and progression of not only HCC and ESCC but also other types of tumors.

Conflicts of interest statement

My co-authors and I declare that we have no proprietary, financial, professional or other personal interest of any nature or kind in any product, service and/or company that could be construed as influencing the position presented in the manuscript entitled, "A novel amplification target, ARHGAP5, promotes cell spreading and migration by negatively regulating RhoA in Huh-7 hepatocellular carcinoma cells".

Acknowledgements

Supported by: Grants-in-Aid for Scientific Research (18390223) from the Japan Society for the Program of Science (to K.Yasui).

References

[1] A. Hall, Rho GTPases and the actin cytoskeleton, Science 279 (1998) 509–514.
[2] P.D. Burbelo, S. Miyamoto, A. Utani, S. Brill, K.M. Yamada, A. Hall, Y. Yamada, P190-B, a new member of the Rho GAP family, and Rho are induced to cluster after integrin cross-linking, J. Biol. Chem. 270 (1995) 30919–30926.
[3] W.T. Arthur, L.A. Petch, K. Burridge, Integrin engagement suppresses RhoA activity via a c-Src-dependent mechanism, Curr. Biol. 10 (2000) 719–722.
[4] G.C. Kennedy, H. Matsuzaki, S. Dong, W.N. Liu, J. Huang, G. Liu, X. Su, M. Cao, W. Chen, J. Zhang, W. Liu, G. Yang, X. Di, T. Ryder, Z. He, U. Surti, M.S. Phillips, M.T. Boyce-Jacino, S.P. Fodor, K.W. Jones, Large-scale genotyping of complex DNA, Nat. Biotechnol. 21 (2003) 1233–1237.
[5] Y. Nannya, M. Sanada, K. Nakazaki, N. Hosoya, L. Wang, A. Hangaishi, M. Kurokawa, S. Chiba, D.K. Bailey, G.C. Kennedy, S. Ogawa, A robust algorithm for copy number detection using high-density oligonucleotide single nucleotide polymorphism genotyping arrays, Cancer Res. 65 (2005) 6071–6079.
[6] Y. Inagaki, K. Yasui, M. Endo, T. Nakajima, K. Zen, K. Tsuji, M. Minami, S. Tanaka, M. Taniwaki, Y. Itoh, S. Arii, T. Okanoue, CREB3L4, INTS3, and SNAPAP are targets for the 1q21 amplicon frequently detected in hepatocellular carcinoma, Cancer Genet. Cytogenet. 180 (2008) 30–36.
[7] K. Yasui, I. Imoto, Y. Fukuda, A. Pimkhaokham, Z.Q. Yang, T. Naruto, Y. Shimada, Y. Nakamura, J. Inazawa, Identification of target genes within an amplicon at 14q12–q13 in esophageal squamous cell carcinoma, Genes Chromosomes Cancer 32 (2001) 112–118.
[8] C. Collins, J.M. Rommens, D. Kowbel, T. Godfrey, M. Tanner, S.I. Hwang, D. Polikoff, G. Nonet, J. Cochran, K. Myambo, K.E. Jay, J. Froula, T. Cloutier, W.L. Kuo, P. Yaswen, S. Dairkee, J. Giovanola, G.B. Hutchinson, J. Isola, O.P. Kallioniemi, M. Palazzolo, C. Martin, C. Ericsson, D. Pinkel, D. Albertson, W.B. Li, J.W. Gray, Positional cloning of ZNF217 and NABC1: genes amplified at 20q13.2 and overexpressed in breast carcinoma, Proc. Natl. Acad. Sci. USA 95 (1998) 8703–8708.
[9] E.A. Cox, S.K. Sastry, A. Huttenlocher, Integrin-mediated adhesion regulates cell polarity and membrane protrusion through the Rho family of GTPases, Mol. Biol. Cell 12 (2001) 265–277.
[10] C. Sakakura, A. Hagiwara, H. Taniguchi, T. Yamaguchi, H. Yamagishi, T. Takahashi, K. Koyama, Y. Nakamura, T. Abe, J. Inazawa, Chromosomal aberrations in human hepatocellular carcinomas associated with hepatitis C virus infection detected by comparative genomic hybridization, Br. J. Cancer 80 (1999) 2034–2039.
[11] Y.J. Chen, J.Y. Ko, P.J. Chen, C.H. Shu, M.T. Hsu, S.F. Tsai, C.H. Lin, Chromosomal aberrations in nasopharyngeal carcinoma analyzed by comparative genomic hybridization, Genes Chromosomes Cancer 25 (1999) 169–175.
[12] T. Yakut, H.J. Schulten, A. Demir, D. Frank, B. Danner, U. Egeli, C. Gebitekin, E. Kahler, B. Gunawan, N. Urer, H. Oztürk, L. Füzesi, Assessment of molecular events in squamous and non-squamous cell lung carcinoma, Lung Cancer 54 (2006) 293–301.
[13] P. Moinzadeh, K. Breuhahn, H. Stützer, P. Schirmacher, Chromosome alterations in human hepatocellular carcinomas correlate with aetiology and histological grade – results of an explorative CGH meta-analysis, Br. J. Cancer 92 (2005) 935–941.
[14] C. Schlaeger, T. Longerich, C. Schiller, P. Bewerunge, A. Mehrabi, G. Toedt, J. Kleeff, V. Ehemann, R. Eils, P. Lichter, P. Schirmacher, B. Radlwimmer, Etiology-dependent molecular mechanisms in human hepatocarcinogenesis, Hepatology 47 (2008) 511–520.
[15] S. Zrihan-Licht, Y. Fu, J. Settleman, K. Schinkmann, L. Shaw, I. Keydar, S. Avraham, H. Avraham, RAFTK/Pyk2 tyrosine kinase mediates the association of p190 RhoGAP with RasGAP and is involved in breast cancer cell invasion, Oncogene 19 (2000) 1318–1328.
[16] G. Chakravarty, D. Roy, M. Gonzales, J. Gay, A. Contreras, J.M. Rosen, P190-B, a Rho-GTPase-activating protein, is differentially expressed in terminal end buds and breast cancer, Cell Growth Differ. 11 (2000) 343–354.
[17] H. Nakahara, S.C. Mueller, M. Nomizu, Y. Yamada, Y. Yeh, W.T. Chen, Activation of beta1 integrin signaling stimulates tyrosine phosphorylation of p190RhoGAP and membrane-protrusive activities at invadopodia, J. Biol. Chem. 273 (1998) 9–12.
[18] X.D. Ren, W.B. Kiosses, M.A. Schwartz, Regulation of the small GTP-binding protein Rho by cell adhesion and the cytoskeleton, EMBO J. 18 (1999) 578–585.
[19] W.T. Arthur, K. Burridge, RhoA inactivation by p190RhoGAP regulates cell spreading and migration by promoting membrane protrusion and polarity, Mol. Biol. Cell 12 (2001) 2711–2720.
[20] K. Takaishi, T. Sasaki, M. Kato, W. Yamochi, S. Kuroda, T. Nakamura, M. Takeichi, Y. Takai, Involvement of Rho p21 small GTP-binding protein and its regulator in the HGF-induced cell motility, Oncogene 9 (1994) 273–279.
[21] A.J. Ridley, P.M. Comoglio, A. Hall, Regulation of scatter factor/hepatocyte growth factor responses by Ras, Rac, and Rho in MDCK cells, Mol. Cell. Biol. 15 (1995) 1110–1122.
[22] C.D. Nobes, A. Hall, Rho GTPases control polarity, protrusion, and adhesion during cell movement, J. Cell Biol. 144 (1999) 1235–1244.

Journal of Medical Virology 80:2069–2078 (2008)

Molecular Characterization of a Variant Virus That Caused De Novo Hepatitis B Without Elevation of Hepatitis B Surface Antigen After Chemotherapy With Rituximab

Masami Miyagawa,[1] Masahito Minami,[1]* Kota Fujii,[1] Rei Sendo,[1] Kojiro Mori,[2] Daisuke Shimizu,[3] Tomoaki Nakajima,[1] Kohichiroh Yasui,[1] Yoshito Itoh,[1] Masafumi Taniwaki,[3] Takeshi Okanoue,[4] and Toshikazu Yoshikawa[1]

[1]*Molecular Gastroenterology and Hepatology, Graduate School of Medical Science, Kyoto Prefectural University of Medicine, Kyoto, Japan*
[2]*Kyoto Prefectural Yosanoumi Hospital, Kyoto, Japan*
[3]*Molecular Hematology and Oncology, Graduate School of Medical Science, Kyoto Prefectural University of Medicine, Kyoto, Japan*
[4]*Saiseikai Suita Hospital, Osaka, Japan*

Hepatitis B virus (HBV) reactivation in hepatitis B surface antigen (HBsAg)-negative patients following treatment with rituximab has been reported increasingly. The aim of this study was to investigate the molecular mechanisms underlying HBV reactivation in an HBsAg-negative patient. HBV was reactivated in a 75-year-old man following chemotherapy with rituximab, without elevation of HBsAg. The patient's full-length HBV genome was cloned and the entire sequence was determined. Transfection studies were performed in vitro using recombinant wild-type HBV (wild-type), the patient's HBV (patient), and two chimeric HBV constructs, in which the preS/S region of the patient and wild-type virus had been exchanged with one another. Secreted HBsAg and intra- and extra-cellular HBV DNA were measured. The number of amino acid substitutions in HBV from this patient was much higher than in previous reports of HBV mutants, such as occult HBV and vaccine escape HBV mutants. Levels of HBsAg and HBV DNA production in vitro were significantly lower in the patient compared to wild-type transfections. From analyses of the chimeric constructs, the altered preS/S region was responsible mainly for this impairment. These results show that highly mutated HBV can reactivate after chemotherapy with rituximab, despite an unusually large number of mutations, resulting in impaired viral replication in vitro. Severe immune suppression, probably caused by rituximab, may permit reactivation of highly mutated HBV. These findings have important clinical implications for the prevention and management of HBV reactivation and may explain partially the mechanism of recent, unusual cases of HBV reactivation. ***J. Med. Virol. 80:2069–2078, 2008.***

KEY WORDS: occult HBV infection; HBV reactivation; mutation; rituximab

INTRODUCTION

Infection with hepatitis B virus (HBV) is a major global public health problem, with 50 million people infected per year and more than 350 million people infected chronically worldwide. HBV infection is associated with a wide spectrum of clinical presentations, ranging from asymptomatic or very mild clinical features to severe liver disease. The majority of acute HBV infections are self-limited, whereas patients with chronic HBV infection generally have persistent infection. In addition, hepatitis B surface antigen (HBsAg)-negative infection or occult HBV infection has been recognized recently [Mrani et al., 2007; Nebbia et al., 2007], but the precise magnitude, pathogenesis, and clinical relevance of these infection are unclear.

*Correspondence to: Masahito Minami, MD, PhD, Molecular Gastroenterology and Hepatology, Graduate School of Medical Science, Kyoto Prefectural University of Medicine, Hirokoji, Kawaramachi, Kamigyo-ku, Kyoto 602-8566, Japan.
E-mail: minami@koto.kpu-m.ac.jp

Accepted 21 July 2008
DOI 10.1002/jmv.21311
Published online in Wiley InterScience (www.interscience.wiley.com)

HBV reactivation in patients who are hepatitis B carriers is well-known and is often a fatal complication of cytotoxic chemotherapy [Yeo et al., 2000]. HBV reactivation diagnosed by HBsAg and anti-HBs titers was first described by Wands et al. [1975]. With the availability of quantitative HBV DNA assays, HBV reactivation can be identified by an increase in HBV DNA titer, and can be related to clinical hepatitis and to the administration of chemotherapy [Lok et al., 1991; Yeo et al., 2000]. To date, many cases of HBV reactivation have been reported in patients with various cancers, such as breast cancer, [Zhong et al., 2004] hepatocellular carcinoma [Yeo et al., 2004] and, in particular, lymphoma [Lok et al., 1991]. Even in cases of resolved HBV infection, HBV DNA may persist in the liver, where its replication is suppressed [Rehermann et al., 1996], but immune suppression may lead to HBV reactivation.

HBV reactivation has been reported to occur in 29–56% of inactive HBsAg carriers that have been treated with chemotherapy [Reff et al., 1994]. Furthermore, a number of HBV reactivations in HBsAg-negative patients have been reported recently. Hui et al. [2006] reported that eight of 244 (3.3%) HBsAg-negative lymphoma patients developed HBV-related hepatitis after chemotherapy. Surprisingly, seven of the eight patients (89%) were treated with a regimen including rituximab. There is little information concerning the molecular mechanism underlying such reactivation and neither complete genome sequencing nor functional analyses of the reactivated HBV have been performed previously.

HBV was reactivated in a person who was negative for both HBsAg and anti-HBs, but positive for anti-HBc. The full length HBV DNA was amplified and complete HBV genome sequencing were undertaken, which is considered suitable for accurate identification of HBV quasi-species. Transfection studies performed with full-length linear HBV, rather than with fragments of the genome, are useful for functional analysis to determine the biological features of the reactivated HBV. The complete sequence of this defective HBV and the expression of HBsAg and replication of the full-length clone in vitro are described.

MATERIALS AND METHODS

Patient

A 75-year-old Japanese man was treated with rituximab, plus cyclophosphamide, adriamycin, vincristine, and prednisone (CHOP), for diffuse large B cell lymphoma. He had never received blood transfusions or hepatitis B vaccine. About 6 months after chemotherapy, he was admitted with elevated levels of serum transaminases. At that time, the blood level of total bilirubin was 0.66 mg/dl, AST was 314 IU/ml, and ALT was 158 IU/ml. The result of HBsAg assay was unusual. Before the onset of hepatitis and the elevation of transaminases, the first screening assay for HBsAg (Fig. 1*1), using a chemiluminescent enzyme immunoassay (Lumipulse II, Fujirebio, Inc., Tokyo, Japan), was negative. However, coinciding with the development of hepatitis, the second HBsAg assay (Fig. 1*2) was positive, but indicated a low titer, whereas the neutralization assay was negative. These contradictory results were interpreted as a false-positive HBsAg assay and the sample was classified as HBsAg-negative at that time. Serological tests for HBV showed that anti-HBs, hepatitis B e antigen (HBeAg), and IgM antibody to HBc antigen (IgM anti-HBc) were all negative, but antibody to HBeAg, total anti-HBc and serum HBV DNA (7.6 log copies/ml) were all positive. In subsequent HBsAg assays, the titer of HBsAg remained low and did not mirror increased HBV DNA levels. For confirmation, therefore, HBsAg was measured using another chemiluminescent immunoassay kit (ARCHITECT, Abbott Japan, Tokyo, Japan), and the result was positive (Fig. 1*3). A needle biopsy performed on the tenth day after admission provided a diagnosis of acute hepatitis. Any recent sexual and iatrogenic contact with HBV was excluded by medical interview and by reviewing treatment history. He had neither a family history of, nor apparent previous infection with HBV. Thus, his hepatitis was considered to result from reactivation of HBV that he had acquired subclinically (Fig. 1). Initially, the patient received lamivudine for 10 days, but serum transaminases increased continuously to 1,400 IU/ml. He was treated with additional steroid and interferon therapy and the hepatitis improved within 2 months.

Full-Length HBV Genome Analysis

HBV DNA was extracted from 200 μl of serum on the tenth day after the patient's admission. Full-length HBV DNA was amplified according to the method described by Günter et al. [1995] with HBV-specific primers, using the Expand high-fidelity PCR system (Roche Diagnostics, Tokyo, Japan). The amplification was performed in an iCycler Thermal Cycler (Bio-Rad Laboratories, Tokyo, Japan) under the following conditions: 94°C for 4 min then, 95°C for 30 sec, 60°C for 30 sec, 72°C for 3 min, for 40 cycles with an increment of 10 sec after each cycle, and 1 cycle of 72°C for 7 min. The PCR products were purified and the full-length HBV genome was cloned using a TOPO TA cloning kit (Invitrogen Japan, Tokyo, Japan). The complete HBV DNA sequences of five clones were determined using appropriate primers.

Genotyping of the HBV DNA sequences was carried out using the CLUSTAL program by phylogenetic comparison along the entire genome with sequences from representative genotypes, A to H. All five HBV clones belonged to genotype C, therefore, the nucleotide and amino acid sequences of HBV DNA isolates were aligned to HBV genotype C (AB033556). The average numbers of mutations in five clones were calculated.

Preparation of Constructs for Transfection

One of the five HBV clones (patient), isolated according to the procedures above, was used as the template plasmid. Another full-length HBV DNA (wild-type) was

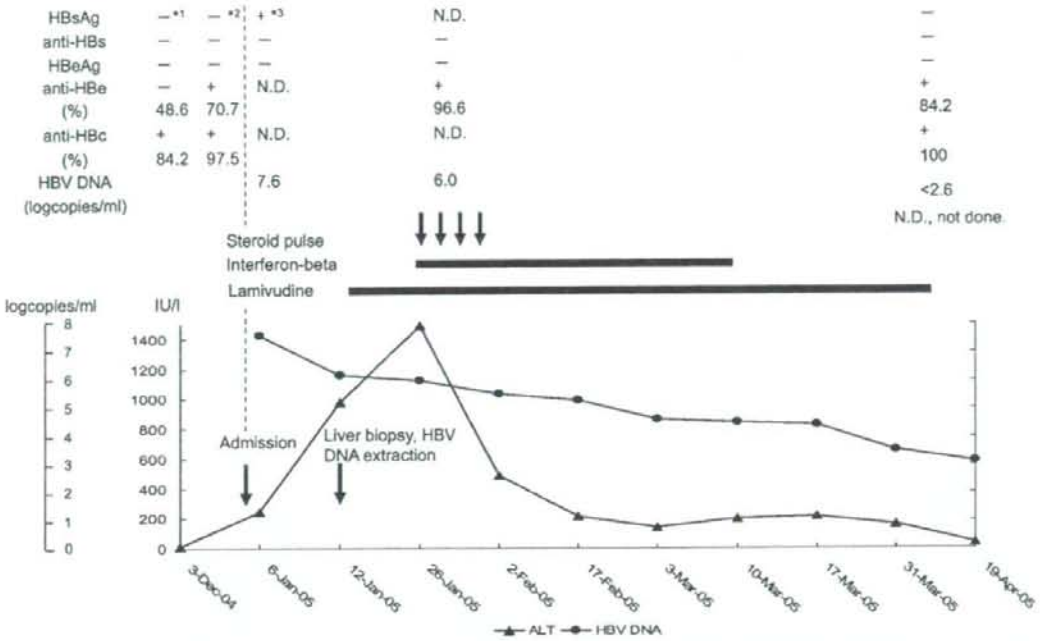

Fig. 1. Serological markers of HBV and clinical course. ALT, alanine aminotransferase. The result of HBsAg assay was unusual. The first screening assay using a chemiluminescent enzyme immunoassay (Lumipulse II, Fujirebio, Inc.) (*1) was negative. The result of the second test was interpreted as a false positive and the sample was classified as HBsAg-negative (*2). For confirmation, HBsAg was measured using another chemiluminescent immunoassay kit (ARCHITECT, Abbott Japan) and the result was positive (*3).

extracted from an HBsAg positive patient, amplified and cloned using the procedures described above, and used as the control plasmid. The sequences encoding the preS/S region were located between *AclI* and *BstEII* restriction sites (Fig. 2). Both plasmids were digested with *AclI* at 37°C for 2 hr, and *BstEII* at 60°C for 2 hr. Plasmids were separated into two fragments; one fragment encoding the preS/S region (1.2 kb) and the other comprising the vector sequence (3.7 kb) ligated to 2.0 kb of HBV DNA without the preS/S region. To construct the chimeric plasmids, the preS/S regions of the patient and the wild-type plasmids were swapped. The structures of the full-length clones are given in Figure 2.

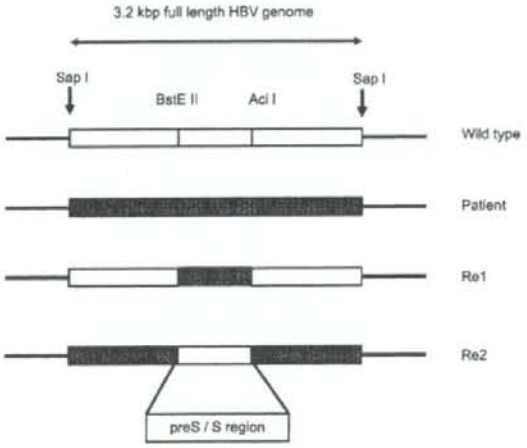

Fig. 2. Structure of HBV DNA transfected into Huh7 cells. Recombinant HBV constructs, Re1 and Re2, were made by exchanging the preS/S regions of the patient and the wild-type clones. The regions in black indicate HBV sequences with mutations. Each full length HBV DNA was cleaved with *SapI* from the vector DNA.

Transfection Study With Full-Length HBV DNA

Transfection of recombinant HBV was performed according to Günter et al. [1995] and Pollicino et al. [2006]. Linear 3.2 kb HBV monomers (patient, wild-type, Re1, Re2) were released from the four plasmids by cleavage with *SapI* (New England Biolabs Japan, Tokyo, Japan). HuH7 human hepatoma cells were plated at a density of 1.3×10^6 cells per 100 mm-diameter culture dish (Falcon, Becton Dickinson and Co., Tokyo, Japan) and incubated for 24 hr to yield 60–90% confluency. The cells were transfected transiently with 5 μg of HBV DNA using Lipofectamine 2000 (Invitrogen Japan). The medium containing DNA was changed 1 day after transfection to stop the reaction, and cells and supernatant were harvested 1 day later.

Transfection efficiency was measured by co-transfection of 1 μg of a reporter plasmid expressing secreted

alkaline phosphatase (TaKaRa BIO, Otsu, Japan). Secreted HBsAg in the culture supernatant was measured by a chemiluminescent immunoassay using a commercially available kit (ARCHITECT, Abbott Japan). HBV DNA was extracted from 200 μl of supernatant. The cells were washed, pelleted by centrifugation, and nucleic acids were extracted from the cell pellet. Quantitation of extracellular and intracellular HBV DNA was undertaken by a real-time PCR method using the SYBR Green I protocol in a Light-Cycler (Roche Diagnostics). Each 20 μl reaction contained 2 μl of Master Mix, 0.5 μM of forward and reverse primers, and 2 μl of sample material. The forward and reverse primers were (637–652) 5′-cctatgggagtgggcctcag-3′ and (742–761) 5′-gcccccaataccacatcatc-3′, which target part of the polymerase region. Amplification was performed as follows: 95°C for 10 min, then 45 cycles of 95°C for 0 sec, 55°C for 0 sec, 72°C for 16 sec. The products were analyzed by fluorescence and crossing point curves, melting curves and electrophoresis. Serial dilutions of a control HBV DNA were used as quantitation standards. HBV constructs without transfection reagent were included as negative controls. All the experiments and measurements were carried out seven times and the mean values were used for analysis.

RESULTS

Nucleotide and Amino Acid Sequence Analysis

All five clones from this patient, as well as the wild-type clone used as the control, belonged to HBV genotype C, according to phylogenetic analysis. Numerous nucleotide mutations were detected in the patient, spread throughout the genome sequence, and some resulted in amino acid substitutions (Table I). In this case, amino acids were changed most frequently within the S region of the surface open reading frame (ORF) (Table I).

Three amino acid substitutions (Q129H, F134Y, D144E) were located in the "a" determinant. The frequency of substitutions in the "a" determinant was almost equal to those reported previously. The subtype of this virus was classified as *ayw* by arginine at position 122 and by lysine at position 160. The remaining 17 amino acid substitutions in the surface ORF were located outside the "a" determinant. No deletions were located within the preS1 and preS2/S promoters, which might lead to reduced secretion of HBsAg [Sengupta et al., 2007].

Besides mutations within the surface ORF, numerous amino acid substitutions were scattered throughout the polymerase ORF. However, no significant amino acid substitutions were detected, which have been reported previously to change the replication ability of the domains [Radziwill et al., 1990; Blum et al., 1991]. No substitution was detected in the YMDD motif.

The core promoter mutations A1762T/G1764T were not found in any isolate. However, the G1896A mutation in the precore region was detected in all isolates.

Functional Analysis of the HBV Genome by Transient Transfection

To investigate the replication capacity and ability of the variant HBV to produce HBsAg in vitro, four constructs (patient, wild-type, Re1 and Re2; Fig. 2) were used for transient transfection of HuH7 cells. HuH7 cells transfected with linear HBV DNA of the patient had accumulated between 40 and 60 HBV molecules per cell 24 hr after transfection, as determined by real-time PCR assay. No HBV DNA or HBsAg were detected in the lysates of cells treated with HBV DNA but without Lipofectamine 2000 transfection regent.

As anticipated, extracellular HBsAg was not detected in the supernatants from cells transfected with the patient clone and was strongly suppressed with the Re1 clone (Fig. 3). Meanwhile, the Re2 clone expressed detectable HBsAg but at a rather lower level than the wild-type.

All four clones were able to release viral DNA into the cell culture medium (Fig. 4). Intracellular and extracellular HBV DNA levels were in proportion for each clone. The level of HBV DNA in the sample transfected with the patient clone was lower than the wild-type level. The secretion of HBV DNA by the patient clone

TABLE I. Position of Amino Acid Substitutions and Number of Mutations in Each Region of the Patient HBV Genome

Location	Position of amino acid mutation	Number of mutations[a] (%)
preS region	F24S (1/5), F45L, N56K, Q80P, D133N, L141E, G149E, T164I,	7.0/174 (4.0%)
S region	E2G, T4I, F8S, Q30S (1/5), T47M, T57I, Y72C (1/5), K122R, T123N, Q129H, F134Y, D144E (3/5), T148I, A159G (3/5), E164D (2/5), V168A, S174N, A184V (1/5), Y206C, Y221C	16.2/226 (7.2%)
Polymerase region	I101V, K127E (1/5), T150S (1/5), F205L (3/5), S213G, I214V, L225P, S237A, W253R, A272S, H277Y, S287P (1/5), V302M, H306N, R313K, F321S, T384I, D477K, I515V (1/5), V519L (2/5), A540T (1/5), F567L (1/5), W589R (1/5), G590D (1/5), L615I, A663S, T718A, E729G (2/5) T743K, L784P (1/5), R807Q, T809S, V830A (1/5), K 841R	23.6/843 (2.8%)
X region	G27R, P36T, D48V, C61R (1/5), E80A, T85A, V92L, S101T/P (2/5,1/5)	6.8/154 (4.4%)
Precore region	W28*	1.0/29 (3.4%)
Core region	E40G (1/5), V115I (1/5), S168T (3/5)	2.0/183 (0.55%)

Mutations within "a" determinant are underlined. Several mutations were detected in one to three of five clones (the number of mutated clone per five clones).
*The number of amino acid mutations per all amino acid in each region. The average number of mutations in five clones was calculated.

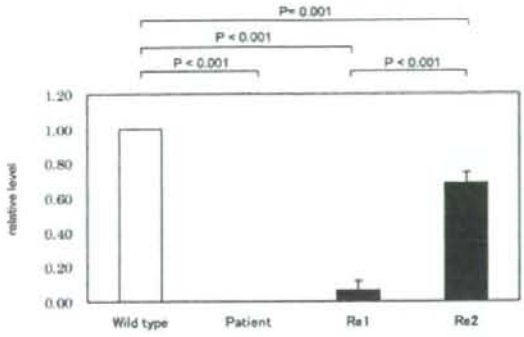

Fig. 3. The expression of HBsAg in cell culture 1 day after transfection. The wild-type clone served as a reference with the value of 1 in the white bar; values of other clones are expressed relative to this in black bars.

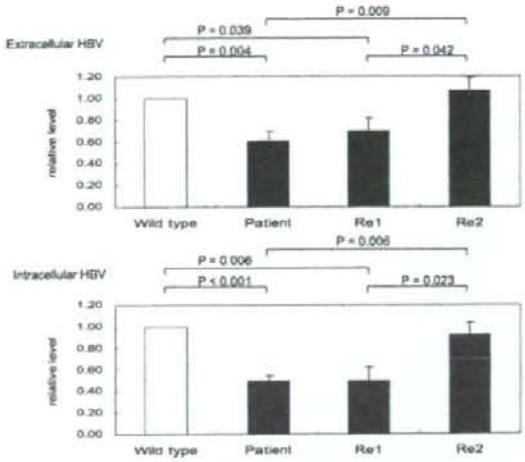

Fig. 4. Extracellular and intracellular expression of HBV DNA measured by real-time PCR. The wild-type clone served as a reference with the value of 1 in the white bar; values of other clones are expressed relative to this in black bars. HBV DNA replication was inhibited from the sample transfected with the HBV construct containing preS/S mutations. The Re2 construct containing the fragment without the mutated S region retains the wild-type replication capacity and produces virions, even though it includes some mutations outside the preS/S region.

and the Re1 clone was suppressed, while the replication of the Re2 clone was comparable to that of the wild-type clone. These results suggest that the altered preS/S sequences in this patient impair not only the synthesis of HBsAg but also the production of HBV DNA and that the mutations outside the preS/S region only weakly inhibit the production of HBsAg.

DISCUSSION

In this study, molecular characterization of an HBsAg-negative, defective HBV that reactivated after CHOP plus rituximab chemotherapy were carried out. There were 812 articles identified from PubMed databases using keywords including "hepatitis" and "reactivation" (Table II). There were 21 reports of HBV reactivations associated with chemotherapy in HBsAg-negative patients and another four reports cited in those articles. Reports associated with transplantations were excluded. In these 25 selected reports, 22 of a total of 36 (61.1%) patients had received chemotherapy containing rituximab [Hui et al., 2006]. Only two studies associated with rituximab treatment [Westhoff et al., 2003; Awerkiew et al., 2007] reported sequencing of the reactivated HBV. These studies revealed approximately five amino acid substitutions within the surface ORF.

The most notable difference between the defective HBV in this case and the mutants reported previously is the large number of mutations and the localization of the mutations within the S region. The number of amino acid substitutions in the S region in this patient was higher than in vaccine-selected HBV mutants and occult HBV reported previously (16.2 vs. 1.0–6.1) (Table III). Only one study, Grethe et al. [1998], reported an unusual variant with similarly high numbers of mutations in the surface ORF (18–23 mutations). It is of note that their case was asymptomatic and had low levels of HBV DNA (10^{2-3} genomes/ml), implying that a highly mutated HBV could not cause active disease under normal host immunity.

By in vitro transfection studies it was found that mutations in the preS/S region abolished HBsAg production. Moreover, mutations outside of the preS/S region may inhibit the secretion of HBsAg partially (Fig. 4, Re2). These findings are in agreement with the view that amino acid substitutions near to but outside of the S region also affect the secretion of HBsAg, as reported by Kreutz [2002].

HBsAg could be detected in vivo only using the immunoassay kit (ARCHITECT, Abbott Japan). This phenomenon is known to occur due to altered antigenicity of HBsAg [Cariani et al., 2007; Gibb et al., 2007]. Low antigenicity of our variant HBsAg was confirmed by in vitro expression assays and by a lower HBsAg titer, in proportion to the level of HBV DNA in vivo. Negative HBsAg detection in vitro may be attributed to lower proliferation efficacy in vitro compared to that in vivo.

Because the sequence of the PreS/S region is overlapped entirely by a large part of the polymerase ORF, the spacer and RT domain, it was determined whether the nucleotide changes in the preS/S region affected the amino acid sequence of the preS/S protein or the polymerase, or both. In the S region, 78.8% of the nucleotide mutations changed the amino acid sequence of only the S protein, while only 5.0% of the mutations were non-synonymous for only the polymerase protein (Fig. 5). Within the region of the preS ORF, 54% of the mutations changed the protein sequence of the polymerase only and 19.8% of these mutations changed the preS domain only (Fig. 5). The mutations within the preS region were considered more likely to change the amino acid sequence of the polymerase than the preS domain of the surface protein.

TABLE II. HBV Reactivation in the HBsAg Negative Patient

References	Pt. no.	Disease	Chemotherapy	HBsAg pre/post	Sequence (mutation)
Dervite et al. [2001]	1	FL	R, CHOP, IFN	N/P	ND
Westhoff et al. [2003]	1	DLCL	R, CHOP	N/P	S region (L110R, R122K, Y/F134S, P142L, D144A)
Tsutsumi et al. [2004]	1	DLBL	R, CHOP	N/P	ND
	1	DLBL	R, CHASE	N/P	ND
Iannitto et al. [2005]	2	CLL	R, A, CHOP, FND	N/P	ND
Law et al. [2005]	1	DLBL	R, CHOP	N/P	ND
Niscola et al. [2005]	1	CLL	R, F	N/N	ND
Scarrecchia et al. [2005]	1	CLL	R	N/N	ND
Hui et al. [2006]	8	L	Contain R, steroid	N/P	ND
Özgönenel et al. [2006]	1	NHL	R, CHOP	N/P	ND
Sera et al. [2006]	1	ML	R, CHOP, CHOP	N/P	ND
Aubourg et al. [2007]	1	L	Contain R, AHSCT	N/P	ND
Awerkiew et al. [2007]	1	NHL	R, CHOP, F, A, R, DHAP	N/P	PreS region (N87K, H117P), S region (G10R, L109R, C137W, G145R)
Yamagata et al. [2007]	1	DLBL	R, CHOP	N/P	ND
Carman et al. [1995]	1	L	Chemotherapy, steroid	N/P	ND
Chalandon et al. [1999]	1	DLBL	Chemotherapy	N/P	ND
Markovic et al. [1999]	1	L	Chemotherapy, steroid	N/P	ND
Senecal et al. [1999]	1	FL	VCAP, BEAM	N/P	ND
Sekine et al. [2000]	1	MLL	Biweekly CHOP	N/P	ND
Franceschini et al. [2001]	1	CLL	F, steroid	N/P	ND
Ishige et al. [2001]	1	AML	BHAC-DMP, BHAC-AMP	N/P	ND
Kawatani et al. [2001]	3	CLL/AML	VP, BHAC-DMP, BHAC-AMP, AraC+MIT	N/P	ND
Marusawa et al. [2001]	1	DLBL	COP	N/N	ND
Alexopoulou et al. [2006a]	1	CLL	F	N/N	S region (T114S, C124N, G130R, N146S, S171F, L175S, G185E)
Alexopoulou et al. [2006b]	1	CLL	F	N/P	ND
Orlando et al. [2006]	1	HCL	2-CdA, IFN	N/P	ND

FL, follicular lymphoma; DLCL, diffuse large-cell lymphoma; DLBL, diffuse large B-cell lymphoma; CLL, chronic lymphocytic leukemia; L, lymphoma; NHL, non-Hodgkin lymphoma; ML, malignant lymphoma; MLL, mixed large-cell lymphoma; AML, acute myelogenous leukemia; HCL, hairy cell leukemia; R, rituximab; CHOP, cyclophosphamide + vincristine + doxorubicin + prednisolone; IFN, Interferon; CHASE, cyclophosphamide + cytarabine + etoposide + dexamethasone; A, alemtuzumab; FND, fludarabine + novantrone + prednisone; F, fludarabine; AHSCT, autologous hematopoietic stem cell transplantation; DHAP, dexamethasone + cisplatin + cytarabine; VCAP, vindesine + cyclophosphamide + adriamycin + prednisone; BEAM, carmustine + etoposide + melphalan + aracytine; BHAC-DMP, daunorubicine + 6-mercaptopurine + enocitabine + prednisolone; BHAC-AMP, daunorubicine + 6-mercaptopurine + enocitabine + prednisolone; VP, vincristine + prednisolone; AraC + MIT, cytarabine + mitoxantrone; COP, cyclophosphamide + vincristine + prednisolone; 2-CdA, 2-chlorodeoxyadenosine; N, negative; P, positive; ND, no data.

TABLE III. The Number of Amino Acid (aa) Mutations in HBV Genomes Isolated From Occult HBV Infection and Vaccine-Escape Mutants

References	Pt. no.	Age	Disease	HBV	Sample	The mean number of aa mutations				
						preS	S	Precore/ core	P	X
This patient	1	75	DLBL	Occ.	Serum	7.0	16.2	2.0	23.6	6.8
Grethe et al. [1998]	1	ND	ASC	Occ.	Serum	ND	21.3	ND	ND	ND
Chaudhuri et al. [2004]	9	18–53	LC, CH	Occ.	Serum	4.9	3.4	4.2	0.6	0.6
Pollicino et al. [2007]	13	50–79	HCC	Occ.	Normal liver	4.5	6.1	10	2.5	5.6
Hou et al. [2001]	20	16–62	CH, blood donors	Occ.	Serum	ND	1.7	ND	ND	ND
Khattab et al. [2005]	4	ND	HCV co-infection	Occ.	Serum	ND	2.4	ND	ND	ND
Datta et al. [2006]	9	22–48	Families of ASC	Occ.	Serum	ND	2.4	ND	ND	ND
Brojer et al. [2006]	5	22–46	Blood donors	Occ.	Plasma	ND	1.4	ND	ND	ND
Protzer-Knolle et al. [1998]	14	38–62	OLT with LC	Vac.	Serum	ND	1.7	ND	ND	ND
Rodriguez-Frias et al. [1999]	5	ND	OLT	Vac.	Serum	ND	4.2	ND	ND	ND
Ijaz et al. [2001]	4	ND	OLT	Vac.	Serum	ND	1.3	ND	ND	ND
He et al. [2001]	4	ND	ASC	Vac.	Serum	ND	1.0	ND	ND	ND
Oon et al. [1995]	16	2–9	HBV carrier children	Vac.	Serum	ND	1.1 ("a")	ND	ND	ND
Hsu et al. [1999]	12	0–12	HBV carrier children	Vac.	Serum	ND	1.4 ("a")	ND	ND	ND
Huang et al. [2004]	5	ND	Vaccinated patients	Vac.	Serum	ND	1.4 ("a")	ND	ND	ND

ND, no date; DLBL, diffuse large B-cell lymphoma; ASC, asymptomatic carrier; LC, liver cirrhosis; CH, chronic hepatitis; HCC, hepatocellular carcinoma; HCV, hepatitis C virus; OLT, orthotopic liver transplantation. Occ., Occult HBV infection, Vac., Vaccine-escape mutant. To compare mutation frequencies between our clone and previous reports, entire HBV or preS/S sequences of HBV were collected from the literatures. Mutations were determined by comparing with genotypes in each report. The average of mutations in these patients was calculated.

It was found that there were 34 amino acid substitutions in the entire polymerase protein. The analysis in vitro demonstrated low replication of the patient's clone (patient), whereas amino acid substitutions in the polymerase outside the preS/S region did not affect HBV DNA production (Re2). Rather, the low replication capacity was presumed to be caused by the mutations located in the part of the polymerase overlapping the preS/S region (Re1) (Fig. 4).

It was found that 11.8 amino acid substitutions within the spacer domain were overlapped by the preS region and 2.4 mutations within the RT domain were overlapped by the S region. Their effects remain unknown and further studies will be needed.

In previous studies, HBV reactivation usually resulted from HBV strains with normal HBsAg production and high replication capacity (Table II). However, in this case, the HBV clones isolated had poor replication ability and produced altered HBsAg. The mutant viruses in this patient, with low replication capacities, persisted probably because they were more fit than wild-type viruses under strong immune pressure before chemotherapy. They benefited presumably from reduced antigen presentation due to low replication, but this needs further investigation. It is of note that a similar phenomenon was reported recently in cases of occult HBV infection [Besisik et al., 2003; Chaudhuri et al., 2004]; lamivudine resistant YMDD mutants, known to have low replication ability, were found occasionally in individuals who had never been treated with lamivudine.

Several cases of fatal HBV reactivation have been reported following rituximab treatment [Czuczman et al., 1999; Ng and Lim, 2001; Coiffier et al., 2002; Skrabs et al., 2002]. More than half of the cases of reported reactivations in HBsAg-negative patients were treated with rituximab-containing chemotherapy (Table II). Rituximab is an engineered chimeric anti-CD20 monoclonal antibody and is used in combination with chemotherapy to treat cases of B-cell non-Hodgkin's lymphoma, in which the CD20 antigen is expressed [Coiffier et al., 2002].

In patients with HBV, not only HBV-specific cytotoxic T lymphocytes, but also B lymphocyte-mediated antigen presentation, are needed to control HBV infection. However, rituximab leads to the depletion of B lymphocytes and results in the failure of antigen-presenting cells to prime the cytotoxic T-lymphocyte responses to HBV [Dai et al., 2004]. Such an immune-compromised state might allow defective HBV to reactivate and cause hepatitis.

In conclusion, it was demonstrated that highly mutated HBV could reactivate after rituximab-containing chemotherapy. To the authors' knowledge, this is the first study to analyze the complete sequence and molecular function of HBV reactivated after administration of rituximab. An unusually large number of mutations resulted in the inhibition of viral replication in vitro, as well as a lack of HBsAg production in vivo and in vitro. From the previous reports, mutated HBV was

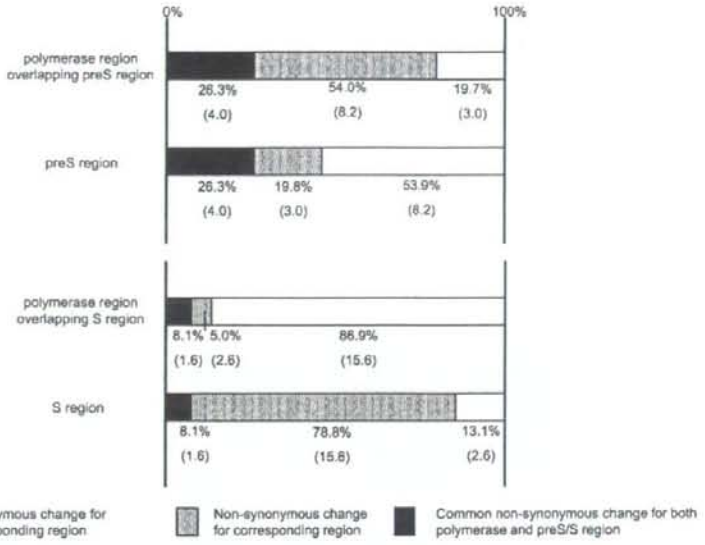

Fig. 5. The rate and number of synonymous and non-synonymous nucleotide changes in preS region, S region and overlapping polymerase region.

detected more frequently after use of rituximab for chemotherapy. Further studies are needed to clarify the frequency and the mechanism of reactivation of defective HBV. These findings have clinical implications for the prevention and management of HBV reactivation; defective HBV can be reactivated even in individuals who are anti-HBc and/or anti-HBs positive and HBV DNA negative. As recommended by others recently [Vitale et al., 2008], it is suggested that monitoring of HBV DNA, as well as HBsAg and anti-HBc, should be carried out, particularly for liver function disorders of unknown origin in patients under an immune-suppressive state after chemotherapy including rituximab.

REFERENCES

Alexopoulou A, Dourakis SP, Pandelidaki H, Archimandritis AJ, Karayiannis P. 2006a. Detection of a hepatitis B surface antigen variant emerging in a patient with chronic lymphocytic leukemia treated with fludarabine. J Med Virol 78:1043–1046.

Alexopoulou A, Theodorou M, Dourakis SP, Karayiannis P, Sagkana E, Papanikolopoulos K, Archimandritis AJ. 2006b. Hepatitis B virus reactivation in patients receiving chemotherapy for malignancies: Role of precore stop-codon and basic core promoter mutations. J Viral Hepat 13:591–596.

Aubourg A, d'Alteroche L, Senecal D, Gaudy C, Bacq Y. 2007. Autoimmune thrombopenia associated with hepatitis B reactivation (reverse seroconversion) after autologous hematopoietic stem cell transplantation. Gastroenterol Clin Biol 31:97–99.

Awerkiew S, Däumer M, Reiser M, Wend UC, Pfister H, Kaiser R, Willems WR, Gerlich WH. 2007. Reactivation of an occult hepatitis B virus escape mutant in an anti-HBs positive, anti-HBc negative lymphoma patient. J Clin Virol 38:83–86.

Besisik F, Karaca C, Akyuz F, Horosanli S, Onel D, Badur S, Sever MS, Danalioghi A, Demir K, Kayamakoglu S, Cakaloglu Y, Okten A. 2003. Occult HBV infection and YMDD variants in hemodialysis patients with chronic HCV infection. Hepatol 38:506–510.

Blum HE, Galun E, Liang TJ, Weizsäcker F, Wand JR. 1991. Naturally occurring missense mutation in the polymerase gene terminating hepatitis B virus replication. J Virol 65:1836–1842.

Brojer E, Grabarczyk P, Liszewski G, Mikulska M, Allain JP, Letowska M. 2006. Characterization of HBV DNA+/HBsAg-blood donors in poland identified by triplex NAT. Hepatology 44:1666–1674.

Cariani E, Pelizzari AM, Rodella A, Gargiulo F, Imberti L, Manca N, Rossi G. 2007. Immune-mediated hepatitis-associated aplastic anemia by the emergence of a mutant hepatitis B virus undetectable by standard assays. J Hepatol 46:743–747.

Carman WF, Korula J, Wallace L, MacPhee R, Mimms L, Decker R. 1995. Fulminant reactivation of hepatitis B due to envelope protein mutant that escaped detection by monoclonal HBsAg ELISA. Lancet 345:1406–1407.

Chalandon Y, Negro F, Hebert D, Dietrich PY. 1999. Watchful monitoring for hepatitis B reactivation after intensive chemotherapy. Ann Oncol 10:483–484.

Chaudhuri V, Tayal R, Nayak B, Acharya SK, Panda SK. 2004. Occult hepatitis B virus infection in chronic liver disease: Full-length genome and analysis of mutant surface promoter. Gastroenterology 127:1356–1371.

Coiffier B, Lepage E, Brière J, Herbrecht R, Tilly H, Bouabdallah R, Morel P, Neste EV, Salles G, Gaulard P, Reyes F, Gisselbrecht C. 2002. CHOP chemotherapy plus rituximab compared with CHOP alone in elderly patients with diffuse large-B-cell lymphoma. N Engl J Med 346:235–242.

Czuczman MS, Grillo-Lopez AJ, White CA, Saleh M, Gordon L, LoBuglio AF, Jonas C, Klippenstein D, Daillaire B, Varns C. 1999. Treatment of patients with low-grade B-cell lymphoma with the combination of chimeric anti-CD20 monoclonal antibody and CHOP chemotherapy. J Clin Oncol 17:268–276.

Dai MS, Chao TY, Kao WY, Shyu RY, Liu TM. 2004. Delayed hepatitis B virus reactivation after cessation of preemptive lamivudine in lymphoma patients treated with rituximab plus CHOP. Ann Hematol 83:769–774.

Datta S, Banerjee A, Chandra PK, Chowdhury A, Chakravarty R. 2006. Genotype, phylogenetic analysis, and transmission pattern of occult hepatitis B virus (HBV) infection in families of asymptomatic HBsAg carriers. J Med Virol 78:53–59.

Dervite I, Hober D, Morel P. 2001. Acute hepatitis B in a patient with antibodies to hepatitis B surface antigen who was receiving rituximab. N Engl J Med 344:68.

Franceschini R, Cataldi A, Tenconi GL, Icardi G, Bruzzone BM. 2001. Reactivation of hepatitis B virus infection during cytotoxic chemotherapy. Am J Gastroenterol 96:606.

Gibb R, Nimmo GR, O'Loughlin P, Lowe P, Drummond D. 2007. Detection of HBsAg mutants in a population with a low prevalence of hepatitis B virus infection. J Med Virol 79:351–355.

Grethe S, Monazahian M, Böhme I, Thomssen R. 1998. Characterization of unusual escape variants of hepatitis B virus isolated from a hepatitis B surface antigen-negative subject. J Virol 72:7692–7696.

Günter S, Li BC, Miska S, Krüger DH, Meisel H, Will H. 1995. Nobel method for efficient amplification of whole hepatitis B virus genomes permits rapid functional analysis and reveals deletion mutants in immunosuppressed patients. J Virol 69:5437–5444.

He C, Nomura F, Itoga S, Isobe K, Nakai T. 2001. Prevalence of vaccine-induced escape mutants of hepatitis B virus in the adult population in China: A prospective study in 176 restaurant employees. J Gastroenterol Hepatol 16:1373–1377.

Hou J, Wang Z, Cheng J, Lin Y, Lau GK, Sun J, Zhou F, Waters J, Karayiannis P, Luo K. 2001. Prevalence of naturally occurring surface gene variants of hepatitis B virus in nonimmunized surface antigen-negative chinese carriers. Hepatology 34:1027–1034.

Hsu HY, Chang MH, Liaw SH, Ni YH, Chen HL. 1999. Changes of hepatitis B surface antigen variants in carrier children before and after universal vaccination in Taiwan. Hepatology 30:1312–1317.

Huang X, Lu D, Ji G, Sun Y, Ma L, Chen Z, Zhang L, Huang J, Yu L. 2004. Hepatitis B virus (HBV) vaccine-induced escape mutants of HBS S gene among children from Qidong area, China. Virus Res 99:63–68.

Hui CK, Cheung WW, Zhang HY, Au WY, Yueng YH, Leung AY, Leung N, Luk JM, Lie AK, Kwong YL, Liang R, Lau GK. 2006. Kinetics and risk of de novo hepatitis B infection in HBsAg-negative patients undergoing cytotoxic chemotherapy. Gastroenterology 131:59–68.

Iannitto E, Minardi V, Calvaruso G, Mulè A, Ammatuna E, Trapani RD, Ferraro D, Abbadessa V, Craxi A, Stefano RD. 2005. Hepatitis B virus reactivation and alemtuzumab therapy. Eur J Haematol 74:254–258.

Ijaz S, Torre F, Tedder RS, Williams R, Naoumov NV. 2001. Novel immunoassay for the detection of hepatitis B surface 'escape' mutants and its application in liver transplant recipients. J Med Virol 63:210–216.

Ishige K, Kawatani T, Suou T, Tajima F, Omura H, Idobe Y, Kawasaki H. 2001. Fulminant hepatitis type B after chemotherapy in a serologically negative hepatitis B virus carrier with acute myelogenous leukemia. Int J Hematol 73:115–118.

Kawatani T, Suou T, Tajima F, Ishiga K, Omura H, Endo A, Ohmura H, Ikuta Y, Idobe Y, Kawasaki H. 2001. Incidence of hepatitis virus infection and severe liver dysfunction in patients receiving chemotherapy for hematologic malignancies. Eur J Haematol 67:45–50.

Khattab E, Chemin I, Vuillermoz I, Vieux C, Mrani S, Guillaud O, Trepo O, Zoulim F. 2005. Analysis of HCV co-infection with occult hepatitis B virus in patients undergoing IFN therapy. J Clin Virol 33:150–157.

Kreutz C. 2002. Molecular, immunological and clinical properties of mutated hepatitis B viruses. J Cell Mol Med 6:113–143.

Law JK, Ho JK, Hoskins PJ, Erb SR, Steinbrecher UP, Yoshida EM. 2005. Fatal reactivation of hepatitis B post-chemotherapy for lymphoma in a hepatitis B surface antigen-negative, hepatitis B core antibody-positive patient: Potential implications for future prophylaxis recommendations. Leuk Lymphoma 46:1085–1089.

Lok AS, Liang RH, Chiu EK, Chan TK, Todd D. 1991. Reactivation of hepatitis B virus replication in patients receiving cytotoxic therapy. Report of a prospective study. Gastroenterology 100:182–188.

Markovic S, Drozina G, Vovk M, Fidler-Jenko M. 1999. Reactivation of hepatitis B but not hepatitis C in patients with malignant lymphoma and immunosuppressive therapy. A prospective study in 305 patients. Hepatogastroenterology 46:2925–2930.

Marusawa H, Imoto S, Ueda Y, Chiba T. 2001. Reactivation of latently infected hepatitis B virus in a leukemia patient with antibodies to hepatitis B core antigen. J Gastroenterol 36:633–636.

Mrani S, Chemin I, Menouar K, Guillaud O, Pradat P, Borghi G, Trabaud MA, Chevallier P, Chevallier M, Zoulim F, Trepo C. 2007. Occult HBV infection may represent a major risk factor of non-response to antiviral therapy of chronic hepatitis C. J Med Virol 79:1075–1081.

Nebbia G, Garcia-Diaz A, Ayliffe U, Smith C, Dervisevic S, Johnson M, Gilson R, Tedder R, Geretti AM. 2007. Predictors and kinetics of occult hepatitis B virus infection in HIV-infected persons. J Med Virol 79:1464–1471.

Ng HJ, Lim LC. 2001. Fulminant hepatitis B virus reactivation with concomitant listeriosis after fludarabine and rituximab therapy: Case report. Ann Hematol 80:549–552.

Niscola P, Principe MD, Maurillo L, Venditti A, Buccisano F, Piccioni D, Amadori S, Poeta GD. 2005. Fulminant B hepatitis in a surface antigen-negative patient with B-cell chronic lymphocytic leukaemia after rituximab therapy. Leukemia 19:1840–1841.

Oon CJ, Lim GK, Ye Z, Goh KT, Tan KL, Yo SL, Hopes E, Harrison TJ, Zuckerman AJ. 1995. Molecular epidemiology of hepatitis B virus vaccine variants in Singapore. Vaccine 13:699–702.

Orlando R, Tosone G, Tiseo D, Piazza M, Portella G, Ciancia R, Martinelli V, Montante B, Rotoli B. 2006. Severe reactivation of hepatitis B virus infection in a patient with hairy cell leukemia: Should lamivudine prophylaxis be recommended to HBsAg-negative, anti-HBc-positive patients? Infection 34:282–284.

Özgönenel B, Moonka D, Savaşan S. 2006. Fulminant hepatitis B following rituximab therapy in a patient with Evans syndrome and large B-cell lymphoma. Am J Hematol 81:302.

Pollicino T, Blloni L, Raffa G, Pediconi N, Squadrito G, Raimondo G, Levrero M. 2006. Hepatitis B virus replication is regulated by the acetylation status of hepatitis B virus cccDNA-bound H3 and H4 histones. Gastroenterology 130:823–837.

Pollicino T, Raffa G, Costantino L, Lisa A, Campello C, Squadrito G, Levrero M, Raimondo G. 2007. Molecular and functional analysis of occult hepatitis B virus isolates from patients with hepatocellular carcinoma. Hepatology 45:277–285.

Protzer-Knolle U, Naumann U, Bartenschlager R, Berg T, Hopf U, Büschenfelde KH, Neuhaus P, Gerken G. 1998. Hepatitis B virus with antigenically altered hepatitis B surface antigen is selected by high-dose hepatitis B immune globulin after liver transplantation. Hepatology 27:254–263.

Radziwill G, Tucker W, Schaller H. 1990. Mutational analysis of the hepatitis B virus P gene product: Domain structure and RNase H activity. J Virol 64:613–620.

Reff ME, Carner K, Chambers KS, Chinn PC, Leonard JE, Raab R, Newman RA, Hanna N, Anderson DR. 1994. Depletion of B-cells in vivo by a chimeric mouse human monoclonal antibody to CD20. Blood 83:435–445.

Rehermann B, Ferrari C, Pasquinelli C, Chisari FV. 1996. The hepatitis B virus persists for decades after patients' recovery from acute viral hepatitis despite active maintenance of a cytotoxic T-lymphocyte response. Nat Med 2:1104–1108.

Rodriguez-Frias F, Buti M, Jardi R, Vargas V, Quer J, Cotrina M, Martell M, Esteban R, Guardia J. 1999. Genetic alterations in the S gene of hepatitis B virus in patients with acute hepatitis B, chronic hepatitis B and hepatitis B liver cirrhosis before and after liver transplantation. Liver 19:177–182.

Scarrecchia C, Cappelli A, Aiello P. 2005. HBV reactivation with fatal fulminanting hepatitis during rituximab treatment in a subject negative for HBsAg and positive for HbsAb and HBcAb. J Infect Chemoter 11:189–191.

Sekine R, Taketazu F, Kuroki M, Takagi S, Imawari M, Kanazawa Y, Kawakami M. 2000. Fatal hepatic failure casued by chemotherapy-induced reactivation of hepatitis B virus in a patient with hematologic malignancy. Int J Hematol 71:256–258.

Senecal D, Pichon E, Dubois F, Delain M, Linassier C, Colombat P. 1999. Acute hepatitis B after autologus stem cell transplantation in a man previously infected by hepatitis B virus. Bone Marrow Transplant 24:1243–1244.

Sengupta S, Rehman S, Durgapal H, Acharya SK, Panda SK. 2007. Role of surface promoter mutations in hepatitis B surface antigen production and secretion in occult hepatitis B virus infection. J Med Virol 79:220–228.

Sera T, Hiasa Y, Michitaka K, Konishi I, Matsuura K, Tokumoto Y, Matsuura B, Kajiwara T, Masumoto T, Horiike N, Onji M. 2006. Anti-HBs-positive liver failure due to hepatitis B Virus Reactivation Induced by rituximab. Intern Med 45:721–724.

Skrabs C, Müller C, Agis H, Mannhalter C, Jäger U. 2002. Treatment of HBV-carrying lymphoma patients with Rituximab and CHOP: A diagnostic and therapeutic challenge. Leukemia 16:1884–1886.

Tsutsumi Y, Tanaka J, Kawamura T, Miura T, Kanamori H, Obara S, Asaka M, Imamura M, Masauzi N. 2004. Possible efficacy of lamivudine treatment to prevent hepatitis B virus reactivation due

to rituximab therapy in a patient with non-Hodgkin's lymphoma. Ann Hematol 83:58–60.

Vitale F, Tramuto F, Orlando A, Vizzini G, Meli V, Cerame G, Mazzucco W, Virdone R, Palazzo U, Villafrate MR, Tagger A, Romano N. 2008. Can the serological status of "Anti-HBc Alone" be considered a sentinel marker for detection of "occult" HBV infection? J Med Virol 80:577–582.

Wands JR, Chura CM, Roll FJ, Maddrey WC. 1975. Serial studies of hepatitisassociated antigen and antibody in patients receiving antitumor chemotherapy for myeloproliferative and lymphoproliferative disorders. Gastroenterology 68:105–112.

Westhoff TH, Jochimsen F, Schmittel A, Stöffler-Meilicke M, Schäfer JH, Zidek W, Gerlich WH, Thiel E. 2003. Fatal hepatitis B virus reactivation by an escape mutant following rituximab therapy. Blood 102:1930.

Yamagata M, Murohisa T, Tsuchida K, Okamoto Y, Tsunoda T, Nakamura M, Kusano K, Majima Y, Kuniyoshi T, Iijima M, Sugaya H, Hiraishi H. 2007. Fulminant B hepatitis in a surface antigen and hepatitis B DNA-negative patient with diffuse large B-cell lymphoma after CHOP chemotherapy plus rituximab. Leuk Lymphoma 48:431–433.

Yeo W, Chan PK, Zhong S, Ho WM, Steinberg JL, Tam JS, Hui P, Leung NW, Zee B, Johnson PJ. 2000. Frequency of hepatitis B virus reactivation in cancer patients undergoing cytotoxic chemotherapy: A prospective study of 626 patients with identification of risk factors. J Med Virol 62:299–307.

Yeo W, Lam KC, Zee B, Chan PS, Mo FK, Ho WM, Wong WL, Leung TW, Chan AT, Ma B, Mok TS, Johnson PJ. 2004. Hepatitis B reactivation in patients with hepatocellular carcinoma undergoing systemic chemotherapy. Ann Oncol 15:1661–1666.

Zhong S, Yeo W, Schroder C, Chan PK, Wong WL, Ho WM, Mo F, Zee B, Johnson PJ. 2004. High hepatitis B virus (HBV) DNA viral load is an important risk factor for HBV reactivation in breast cancer patients undergoing cytotoxic chemotherapy. J Viral Hepat 11:55–59.

Hepatology Research 2008; **38**: 886–895 doi: 10.1111/j.1872-034X.2008.00324.x

Original Article

Activation of B-Myb by E2F1 in hepatocellular carcinoma

Tomoaki Nakajima,[1] Kohichiroh Yasui,[1] Keika Zen,[1] Yoshikazu Inagaki,[1] Hideki Fujii,[1] Masahito Minami,[1] Shinji Tanaka,[2] Masafumi Taniwaki,[3] Yoshito Itoh,[1] Shigeki Arii,[2] Johji Inazawa[4] and Takeshi Okanoue[1]

[1]*Molecular Gastroenterology and Hepatology,* [3]*Molecular Hematology and Oncology, Graduate School of Medical Science, Kyoto Prefectural University of Medicine, Kyoto,* [2]*Department of Hepato-Biliary-Pancreatic Surgery, and* [4]*Department of Molecular Cytogenetics, Medical Research Institute, Tokyo Medical and Dental University, Tokyo, Japan*

Aim: Deregulation of E2F1 transcriptional activity is observed in a variety of cancers, including hepatocellular carcinoma (HCC). The aim of the present study is to identify transcriptional target genes of E2F1 in HCC.

Methods: We determined expression levels for *E2F1* and ten candidate genes thought to be targets of E2F1 in primary HCCs using a real-time quantitative reverse transcription-PCR assay. Following small interfering RNA (siRNA)-mediated knockdown of *E2F1* in HCC cell lines, we quantified mRNA levels of the candidate E2F1 target genes.

Results: *E2F1* was significantly over-expressed in 41 primary HCCs as compared to non-tumorous liver tissues. Among the candidates, *MYBL2*, whose product is the transcriptional factor B-Myb, which is involved in controlling cell-cycle progression and apoptosis, was significantly over-expressed in primary HCCs. Additionally, expression levels of *MYBL2* correlated with those of *E2F1*. Knockdown of *E2F1* resulted in a decrease in expression of *MYBL2*. A copy-number gain for *MYBL2* was observed in 36 of 66 primary HCCs, suggesting that *MYBL2* expression is up-regulated by amplification in addition to being regulated by E2F1. Moreover, siRNA-mediated knockdown of *MYBL2* led to reduced expression of *CDC2* (which encodes CDC2), cyclin A2 (*CCNA2*), and topoisomerase II α (*TOP2A*), implicating these genes in the cell cycle and suggesting that they may be downstream targets of B-Myb.

Conclusion: *MYBL2* is a probable transcriptional target of E2F1 in HCC and may therefore be a useful biomarker for diagnosis and an attractive target for molecular therapies useful to treat HCC.

Key words: CCNA2, CDC2, E2F1, hepatocellular carcinoma, MYBL2, TOP2A

INTRODUCTION

HEPATOCELLULAR CARCINOMA (HCC) is the fifth most common malignancy in the world and is estimated to result in approximately half a million deaths annually.[1] Several risk factors for HCC have been reported, including infection with hepatitis B virus (HBV), hepatitis C virus (HCV), dietary aflatoxin, alcohol consumption, and diabetes.

Deregulation of E2F transcriptional activity as a result of alterations in the $p16^{INK4a}$-cyclin D1-Rb pathway is a hallmark of human cancer. E2Fs comprise a family of related factors that control the expression of genes important for cell-cycle progression as well as other processes such as apoptosis, DNA repair, and differentiation.[2,3] There are now eight known human E2F family genes: *E2F1-E2F8*. The E2F1 through to E2F6 proteins dimerize with one of three DP proteins (DP1, DP2/3, or DP4) to form functional transcriptional factor complexes that can bind DNA with high affinity. The function of the E2F-DP heterodimer is thought to be determined primarily by which E2F is present in the heterodimeric complex.

Our earlier studies identified *TFDP1*, which encodes DP1, as a probable target within a 13q34 amplicon that is frequently detected in HCCs[4] and esophageal squamous cell carcinomas.[5] Elevated expression of *TFDP1* was associated with large HCC tumor size and down-regulation of *TFDP1* inhibited growth of HCC cells.[6]

Correspondence: Dr Kohichiroh Yasui, Molecular Gastroenterology and Hepatology, Graduate School of Medical Science, Kyoto Prefectural University of Medicine, Kyoto, 465 Kajii-cho, Kamigyo-ku, Kyoto 602-8566, Japan. Email: yasuik@koto.kpu-m.ac.jp
Received 12 November 2007; revision 13 December 2007; accepted 13 December 2007.

Amplification of *E2F1* has been reported in some cancer cell lines and *E2F1* may be a target for the chromosome 20q amplification.[7] High levels of E2F1 in cancers of the lung, breast, and pancreas correlate with poor clinical outcomes.[2] In contrast, reduced E2F1 expression in colon cancer and bladder cancer correlates with more aggressive malignancy. Paradoxically, E2F1 has been shown to have the ability to induce both cell-cycle progression and programmed cell death, potentially leading to both tumor-promoting and tumor-suppressing effects.[7] Deregulation of E2F1 expression can lead to promotion or inhibition of tumorigenesis, depending on what other oncogenic mutations are present.[2]

B-Myb belongs to the Myb family of transcriptional factors, which include A-Myb and C-Myb.[8] Whereas A-Myb and C-Myb are tissue-specific, B-Myb is expressed ubiquitously. B-Myb plays an important role in the cell cycle and in cell survival.[8,9] *MYBL2*, which encodes B-Myb, is induced by E2F1.[10] B-Myb expression is barely detectable in G0 and is induced at the G1/S transition of the cell cycle.[8] The broad expression of B-Myb in proliferating cells at least in part explains the phenotype of B-Myb knockout mice; that is, death in early embryogenesis.[11]

Herein we examined *E2F1* expression in HCC and explored transcriptional targets of E2F1 that are activated in this type of tumor. Intriguingly, *MYBL2* emerged as a likely downstream target of E2F1. Further, we show that B-Myb protein can activate expression of genes that encode CDC2, cyclin A2, and topoisomerase II α, which are required for cell cycle progression.

METHODS

Cell lines and tumor samples

A TOTAL OF 21 liver cancer cell lines were examined in this study: HCC-derived HLE;[12] HLF;[12] PLC/PRF/5; Li7;[13] Huh7; Hep3B; SNU354;[14] SNU368;[14] SNU387;[14] SNU398;[14] SNU423;[14] SNU449;[14] SNU475;[14] JHH-1;[15] JHH-2;[15] JHH-4;[15] JHH-5;[15] JHH-6;[15] JHH-7;[15] Huh-1;[16] and the hepatoblastoma line HepG2. All cell lines were maintained in Dulbecco's modified Eagle's medium (DMEM) supplemented with 10% fetal bovine serum. We obtained a total of 66 primary HCC tumors from patients undergoing surgery at the Tokyo Medical and Dental University and Kyoto University. Before initiation of the present study, informed consent was obtained in the formal style approved by all relevant ethical committees. Genomic DNA was isolated from each cell line and from primary tumors using the Puregene DNA isolation kit (Gentra, MN, USA). Total RNA could be extracted from 41 of these primary HCCs.

Fluorescence *in situ* hybridization (FISH)

We performed FISH using as a probe the bacterial artificial chromosome (BAC) RP11-73E4, which includes *MYBL2*, as described previously.[4] Briefly, the probe was labeled by nick translation with biotin-16-dUTP (Roche Diagnostics, Germany) and hybridized to metaphase chromosomes. Hybridization signals for biotin-labeled probes were detected with avidin-fluorescein (Roche Diagnostics).

Real-time PCR

We quantified genomic DNA and mRNA by real-time fluorescence detection. Total RNA was obtained using Trizol (Invitrogen, CA, USA). Residual genomic DNA was removed by incubating the RNA samples with RNase-free DNase I (Takara Bio, Japan) prior to reverse transcription (RT)-PCR. Single-stranded complementary DNA (cDNA) was generated using Superscript III Reverse Transcriptase (Invitrogen) following the manufacturer's directions. Real-time quantitative PCR experiments were performed with the LightCycler system using Faststart DNA Master Plus SYBR Green I (Roche Diagnostics) according to the manufacturer's protocol. Primer sequences are listed in supplementary Tables S1 and S2. *GAPDH*[17] and long interspersed nuclear element-1 (LINE-1)[18] were used as endogenous controls for mRNA and genomic DNA levels, respectively.

RNA interference studies

For RNA interference (RNAi), small interfering RNA (siRNA) duplex oligoribonucleotides targeting *E2F1* or *MYBL2*, along with a non-silencing control siRNA which has no significant similarity to any known mammalian gene, were obtained from Qiagen (Japan). The siRNAs were delivered into JHH-5 cells using Hyperfect transfection reagent (Qiagen) according to the manufacturer's instructions. To determine mRNA levels, cells were harvested 48 h after transfection and subjected to real-time quantitative RT-PCR as described above.

Statistical analysis

All statistical analyses were performed using SPSS version 15.0 (SPSS, IL, USA). Either the Wilcoxon signed-rank test or the Mann–Whitney *U*-test was used to compare mRNA levels among tumorous and non-tumorous tissues. Any apparent associations were tested via Pearson's correlation coefficient analysis. χ^2-tests

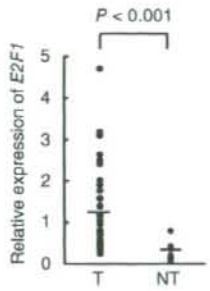

Figure 1 Over-expression of *E2F1* in primary hepatocellular carcinoma (HCC). Relative expression levels of *E2F1* in 41 primary HCC tumors (T) and seven non-tumorous liver tissues (NT) were evaluated by real-time quantitative RT-PCR and normalized to *GAPDH*. Horizontal lines indicate the means of expression levels.

were used to evaluate associations between clinicopathological parameters and the level of *MYBL2* expression. *P* values of <0.05 were considered significant.

RESULTS

Identification of E2F1 downstream genes

WE DETERMINED THE levels of *E2F1* mRNA in 41 primary HCCs and seven non-tumorous liver tissues using real-time quantitative RT-PCR. *E2F1* was significantly over-expressed in HCC tumors as compared to non-tumorous tissues (Mann–Whitney *U*-test, $P < 0.001$; Fig. 1).

To identify genes induced by E2F1 in HCC, we examined ten candidate genes thought to be targets of E2F1: *MYBL2* (which encodes B-Myb); *CDC2* (CDC2/CDK1); *CCNA2* (cyclin A2); *CCNE1* (cyclin E); *MYC* (c-MYC); *DHFR* (dihydrofolate reductase); *TYMS* (thymidylate synthetase); *TK1* (thymidine kinase 1); *RRM1* (ribonucleotide reductase M1); and *PCNA* (proliferating cell nuclear antigen). For this purpose, we knocked down expression of *E2F1* via siRNA. In HCC-derived JHH-5 cells that received siRNA targeting *E2F1*, we observed a decrease in *E2F1* mRNA levels relative to what was observed for cells that received a control siRNA or for untreated cells (Fig. 2A). Following siRNA-mediated knockdown of *E2F1*, we quantified mRNA levels of the ten candidate genes. Knockdown of *E2F1* led to a decrease in expression of *MYBL2*, *CCNE1*, *MYC*, *TK1*, and *RRM1*, but not *CDC2*, *CCNA2*, *DHFR*, *TYMS*, or *PCNA* (Fig. 2A).

We next determined the expression levels of the ten candidate genes in 41 primary HCCs and seven non-tumorous liver tissues. Real-time quantitative RT-PCR analyses revealed that *MYBL2*, *CDC2*, and *CCNA2* were significantly over-expressed in HCC tumors as compared to non-tumor tissues (Fig. 2B). Among the ten candidates, only *MYBL2* was down-regulated following siRNA-mediated knockdown of *E2F1* and significantly over-expressed in primary HCCs. Therefore, we chose to further analyze *MYBL2*, which encodes the transcriptional factor B-Myb.

To further test if over-expression of *MYBL2* correlates with primary HCC tumors, we quantified *MYBL2* expression in paired tumor and non-tumor tissues from an additional 22 patients with HCC. *MYBL2* was significantly over-expressed in 20 (91%) of the tumors as compared to their non-tumorous counterparts (Wilcoxon signed-rank test, $P < 0.001$; Fig. 2C). Further, the expression of *MYBL2* significantly correlated with those of *E2F1* in the 22 primary HCC tumors (Fig. 2D) and in the 21 HCC cell lines (Fig. 2E). Taken together, these observations indicate that *MYBL2* is up-regulated in HCC and is a probable transcriptional target of E2F1.

To clarify the relationship between expression of *MYBL2* and various clinicopathological parameters, we

Figure 2 *MYBL2* is up-regulated in hepatocellular carcinoma (HCC) and is a probable transcriptional target of *E2F1*. (A) siRNA-mediated knockdown of *E2F1* in HCC cell lines. JHH-5 cells were treated with 5 nM siRNA targeting *E2F1* (si*E2F1*) or control siRNA (non-silencing) and harvested 48 h after transfection. Untreated cells were maintained under identical experimental conditions. Relative expression of *E2F1* and its ten putative downstream genes was evaluated by real-time quantitative RT-PCR. Results are presented as the ratio between expression of each gene and a reference gene (*GAPDH*) to correct for variation in the amount of RNA. Relative expression levels were normalized such that for untreated cells, this ratio is 1. (B) Expression of ten putative *E2F1*-downstream genes in 41 primary HCC tumors (T) relative to expression in seven non-tumorous liver tissues (NT). Horizontal lines indicate the means of expression levels. (C) Relative expression of *MYBL2* in paired tumor (T) and non-tumor (NT) tissues from 22 patients with HCC. (D, E) Correlation between expression levels of *E2F1* and *MYBL2* in 22 primary HCC tumors (D) and 21 HCC cell lines (E). Pearson's correlation coefficient analysis revealed that there was a significant correlation between expression levels of the two genes. (□) untreated, (▨) non-silencing, (■) siE2F1.